JACS
JOURNAL OF THE AMERICAN CHEMICAL SOCIETY
Article
pubs.acs.org/JACS

Unquenchable Surface Potential Dramatically Enhances Cu^{2+} Binding to Phosphatidylserine Lipids

Xiao Cong,[†] Matthew F. Poyton,[‡] Alexis J. Baxter,[‡] Saranya Pullanchery,[‡] and Paul S. Cremer*[,‡,§]

[†]Department of Chemistry, Texas A&M University, College Station, Texas 77843, United States
[‡]Department of Chemistry, [§]Department of Biochemistry and Molecular Biology, Penn State University, University Park, Pennsylvania 16802, United States

Supporting Information

ABSTRACT: Herein, the apparent equilibrium dissociation constant, K_{Dapp}, between Cu^{2+} and 1-palmitoyl-2-oleoyl-*sn*-glycero-3-phospho-L-serine (POPS), a negatively charged phospholipid, was measured as a function of PS concentrations in supported lipid bilayers (SLBs). The results indicated that K_{Dapp} for Cu^{2+} binding to PS-containing SLBs was enhanced by a factor of 17 000 from 110 nM to 6.4 pM as the PS density in the membrane was increased from 1.0 to 20 mol %. Although Cu^{2+} bound bivalently to POPS at higher PS concentrations, this was not the dominant factor in increasing the binding affinity. Rather, the higher concentration of Cu^{2+} within the double layer above the membrane was largely responsible for the tightening. Unlike the binding of other divalent metal ions such as Ca^{2+} and Mg^{2+} to PS, Cu^{2+} binding does not alter the net negative charge on the membrane as the $Cu(PS)_2$ complex forms. As such, the Cu^{2+} concentration within the double layer region was greatly amplified relative to its concentration in bulk solution as the PS density was increased. This created a far larger enhancement to the apparent binding affinity than is observed by standard multivalent effects. These findings should help provide an understanding on the extent of Cu^{2+}–PS binding in cell membranes, which may be relevant to biological processes such as amyloid-β peptide toxicity and lipid oxidation.

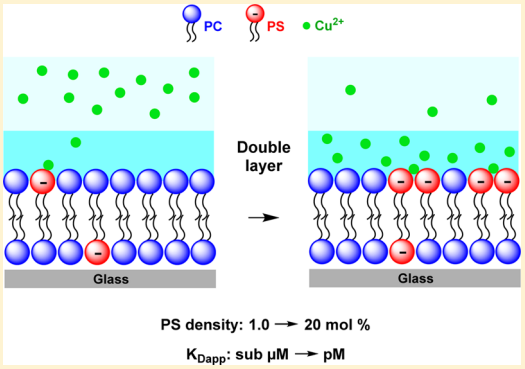

INTRODUCTION

Ligand–receptor interactions on cell membranes underlie many fundamental biological processes such as cell signaling, pathogen recognition, and inflammatory response.[1−4] In multivalent binding systems, a higher surface concentration of membrane receptors not only provides more sites for interactions but may also increase binding avidity and induce receptor clustering.[1,4,5] Curiously, increasing the surface density of receptors typically leads to only modest changes in binding avidity.[1,2,5,6] One example is the bivalent interaction between lipid membrane-conjugated haptens and antibodies. For this system, the apparent equilibrium dissociation constant, K_{Dapp}, tightened by a factor of 12 as the ligand density was increased sufficiently to switch the binding mode from predominantly monovalent to overwhelmingly bivalent.[5] For bivalent binding at interfaces, it can be shown that K_{Dapp} varies with membrane receptor density $[R]_s$, which has units of mol/m^2 (eq 1).[5] The individual dissociation constants, K_{D1} and K_{D2}, for this two-step binding process can be described by eqs 2 and 3, where [B] represents the concentration of bivalent ligands at equilibrium.[5]

$$K_{Dapp} = \frac{K_{D1}K_{D2}}{K_{D2} + 2[R]_S} \quad (1)$$

$$K_{D1} = \frac{[B][R]_S}{[BR]_S} \quad (2)$$

$$K_{D2} = \frac{[BR]_S[R]_S}{[BR_2]_S} \quad (3)$$

The change in K_{Dapp} as a function of $[R]_s$ can be fit to eq 1 to abstract the K_{D1} and K_{D2} values.[5] If $K_{D2} \gg [R]_s$, there is almost no change in K_{Dapp} even with a 20-fold increase in $[R]_s$. Conversely, if $K_{D2} \ll [R]_s$, then a 20-fold increase in membrane receptor density leads to a 20-fold change in K_{Dapp}, the maximum possible.

Increasing the interfacial charge can also modulate the apparent dissociation constant for charged membrane-binding proteins.[7] The surface charge can be tuned by modulating the pH or increasing the number of charged ligands at the surface. When this occurs, the concentration of oppositely charged analytes builds up in the double layer above the membrane surface.[8] This tuning of interfacial charge typically leads to only about an order of magnitude tightening in the K_{Dapp} value as the surface charge on the membrane is rapidly quenched when oppositely charged proteins, peptides, or ions become bound.[7,9]

Received: March 30, 2015
Published: June 11, 2015

DOI: 10.1021/jacs.5b03313
J. Am. Chem. Soc. 2015, 137, 7785−7792

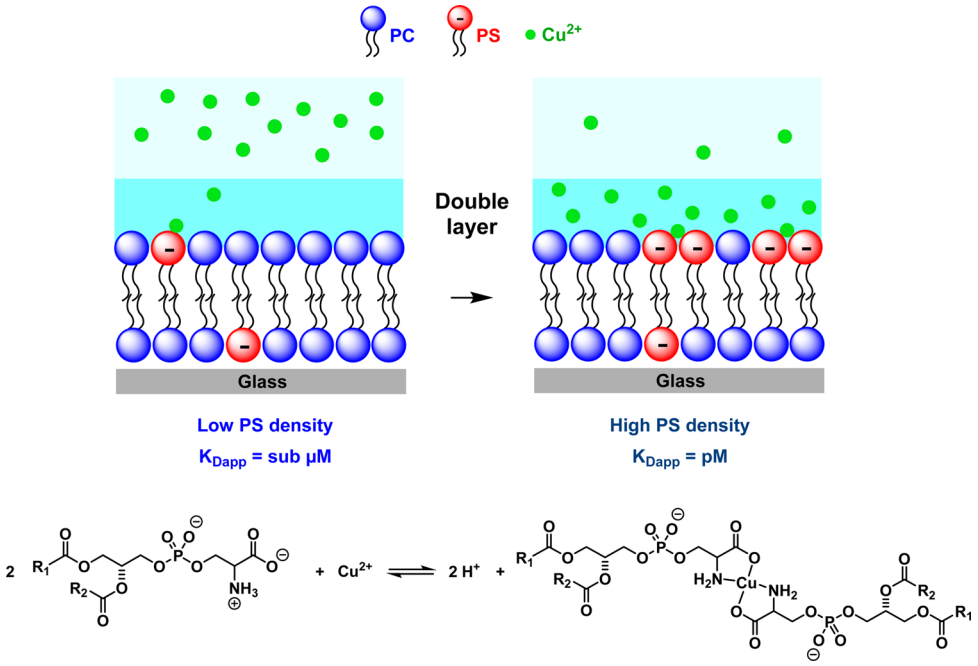

Figure 1. (Top) Schematic representation of the change of K_{Dapp} with PS density in SLBs and (bottom) the binding reaction for Cu^{2+} with two PS molecules.

In fact, most effects of ligand density, ligand presentation, and modulation of the surface charge at membrane interfaces are only moderately impactful to the apparent dissociation constant.[1,10−12] A Coulombic effect could, however, cause the apparent dissociation constant of a charged analyte to change much more drastically if the surface potential remained unquenched upon ligand−receptor binding.

As one of the most abundant negatively charged phospholipids in human membranes, PS plays important roles in cell apoptosis, blood clotting, and embryonic development.[13−17] PS has long been known to form complexes with metal ions such as Ca^{2+} and Mg^{2+}.[18−21] These interactions are assumed to be relatively weak with K_{Dapp} values generally measured to be 10^{-3} M or weaker.[9,18,20] Despite an abundance of studies on Ca^{2+}−PS binding, there is far less known about how PS interacts with transition metal ions and how these interactions manipulate the distribution and function of PS in the membrane.[19,22]

Herein, we demonstrate that the apparent dissociation constant between Cu^{2+} and POPS is highly sensitive to PS density in the membrane. Strikingly, the K_{Dapp} value of Cu^{2+} for POPS in SLBs tightened by a factor of 17,000 when the POPS density was increased from 1.0 mol % to 20 mol %. This change is significantly larger than what would be expected for merely changing from monovalent to predominantly bivalent binding.[5,6] Rather, this dramatic increase in affinity is largely caused by the increased charge on the membrane, which leads to an increase in Cu^{2+} concentration in the double layer (Figure 1). The binding of Cu^{2+} to PS causes little attenuation in the surface potential, unlike other bivalent metal ions such as Ca^{2+} and Mg^{2+} which neutralize or even reverse the surface potential upon binding.[9,18,20] This is a result of the deprotonation of two PS molecules upon the bivalent binding of Cu^{2+} (Figure 1). These results may have implications for Cu^{2+}−PS interactions in cellular membranes, where the PS concentration on the outer leaflet of the plasma membrane increases dramatically upon apoptosis.[13,15]

RESULTS

Cu^{2+}−PS Fluorescence Quenching Assay. A fluorescence quenching assay, which was performed inside microfluidic devices, was used to make the binding measurements described below. As reported previously, the quenching phenomenon can be ascribed to the formation of a complex between Cu^{2+} and PS, which in turn quenches a membrane-bound dye molecule.[22] The experimental setup is shown schematically in Figure S1. To measure the Cu^{2+} binding affinity at different POPS concentrations, vesicle solutions containing 0 to 20 mol % POPS, 1.0 mol % Texas Red 1,2-dihexadecanoyl-*sn*-glycero-3-phosphoethanolamine (TR-DHPE), and 1-palmitoyl-2-oleoyl-*sn*-glyero-3-phosphocholine (POPC) were incubated inside a parallel array of microfluidic channels to form SLBs. Buffer solutions containing different Cu^{2+} concentrations were introduced into each channel and flowed continuously until the fluorescence signal stabilized. Figure 2 shows (A) fluorescence images and (B) the corresponding line scans of SLBs containing 0, 5.0, 10, 15, and 20 mol % POPS without (left) and with (right) 10 nM $CuCl_2$ in the buffer. The fluorescence intensity of each channel was essentially identical in the absence of Cu^{2+}. Upon introducing 10 nM $CuCl_2$ into the solution, the fluorescence of TR-DHPE was quenched to a significantly greater extent at higher POPS concentrations. Specifically, the fraction of the fluorescence that was quenched was 0.86 at 20 mol % POPS, but only 0.56 with 5.0 mol % POPS. As will be discussed below, such changes are the result of two factors, the tightening of the K_{Dapp} value between Cu^{2+} and POPS at higher PS concentrations as well as the shorter average distance between Cu^{2+}−PS complexes and the fluorophores.

Noncompetitive Binding Measurement. In the next set of experiments, multichannel microfluidic devices were used to measure binding isotherms of Cu^{2+} to POPS in supported bilayers containing 1.0 to 7.5 mol % POPS (Figure 3). This was done by monitoring the fraction of fluorescence quenched at

DOI: 10.1021/jacs.5b03313
J. Am. Chem. Soc. 2015, 137, 7785−7792

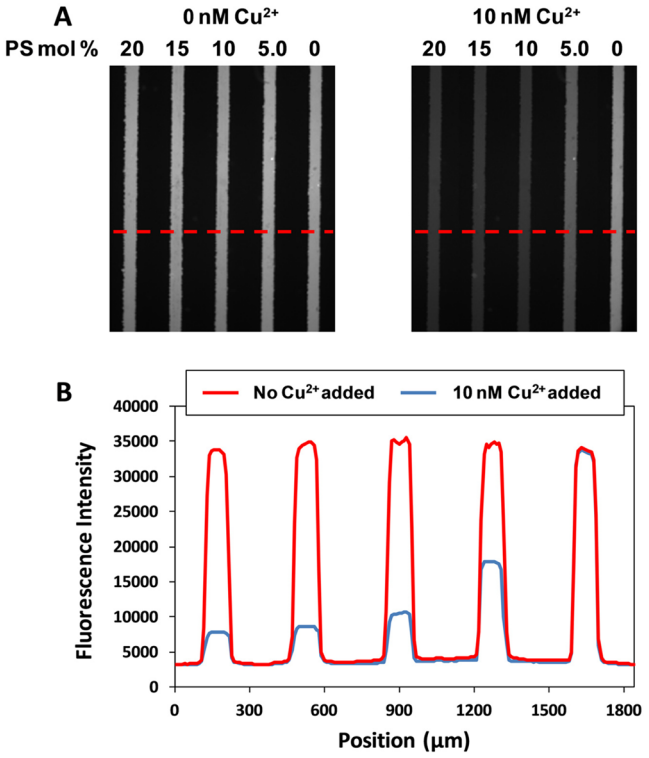

Figure 2. (A) Fluorescence images and (B) line scans from microfluidic devices with 0 to 20 mol % POPS in POPC SLBs along with 1.0 mol % TR-DHPE. The fluorescence is shown in the absence of $CuCl_2$ (left panel in A and red line scan in B) and in the presence of 10 nM $CuCl_2$ (right panel in A and blue line scan in B) at pH 7.4 with 10 mM Tris buffer. The fluorescence line scans in B were taken along the regions with the dotted red lines shown in A. Besides POPS, other PS with different acyl chains such as DPPS and DOPS in POPC SLBs were also tested and they showed similar binding affinity to Cu^{2+} (Figure S2).

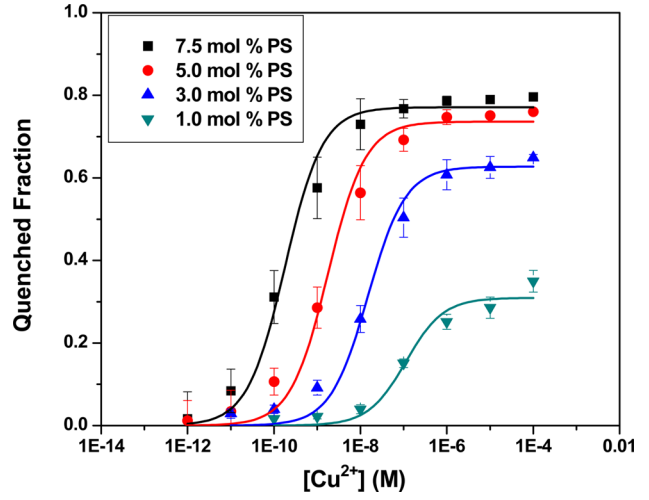

Figure 3. Quenching response of SLBs composed of 1.0 mol % TR-DHPE in POPC with 1.0 to 7.5 mol % POPS as a function of $CuCl_2$ concentration. The experiments were conducted at pH 7.4. The fluorescence intensities in the presence of different Cu^{2+} concentrations were normalized to the fluorescence response without Cu^{2+} in 400 μM EDTA. The fraction of fluorescent dye that was quenched (one minus the normalized fluorescence intensity) is plotted in the figure as a function of Cu^{2+} concentration along with a solid line fit of the data to eq 4

each mol % POPS as a function of $CuCl_2$ concentration in the bulk solution. The maximum fraction of fluorophores that were quenched was found to increase by almost a factor of 3 with increasing POPS concentration. This is expected as the average distance between Cu^{2+}–PS complexes and fluorophores becomes shorter at higher complex concentrations and, therefore, the quenching becomes more efficient.[23] More significantly, these curves revealed tighter binding between Cu^{2+} and POPS as the concentration of the latter was increased. The data were fit to Langmuir isotherms using eq 4 in order to abstract the apparent equilibrium dissociation constant, K_{Dapp}, at each POPS concentration:[5,24,25]

$$\Delta F = \Delta F_{max} \times \frac{[Cu^{2+}]}{[Cu^{2+}] + K_{Dapp}} \quad (4)$$

In this equation, ΔF is the fraction of lipid-bound dye molecules that were quenched by the Cu^{2+}–PS complex at each Cu^{2+} concentration, while ΔF_{max} represents the maximum fraction quenched at the saturation concentration. $[Cu^{2+}]$ represents the free Cu^{2+} concentration in the bulk solution when equilibrium was established. It should be noted that a buffer containing $CuCl_2$ was continuously flowed over the SLBs throughout the experiment so that the bulk Cu^{2+} concentration was not depleted when equilibrium was established. Moreover, equilibrium was determined to have been achieved when the fluorescence response from the membrane stopped changing as a function of time as the buffer was flowed. The values of K_{Dapp} determined at each POPS concentration in Figure 3 are listed in the K_{Dapp} (M, noncompetitive) column of Table 1.

Table 1

PS mol % in SLBs	K_{Dapp} (M, noncompetitive)	K_{Dapp} (M, competitive)	K_{Dcom} (M)
1.0	1.1×10^{-7}	–	–
3.0	1.5×10^{-8}	–	–
5.0	2.7×10^{-9}	–	–
7.5	1.8×10^{-10}	5.1×10^{-11}	5.1×10^{-6}
10	–	1.6×10^{-11}	1.6×10^{-6}
15	–	9.7×10^{-12}	9.7×10^{-7}
20	–	6.4×10^{-12}	6.4×10^{-7}

Competitive Binding Measurements. Binding curves could not be established for SLBs containing more than 7.5 mol % POPS because the value of K_{Dapp} continued to tighten and quenching measurements needed to be made with ever lower concentrations of $CuCl_2$ in the buffer. This was problematic because trace Cu^{2+} contamination in the buffer began to affect the results as the K_{Dapp} value continued to tighten. Therefore, it was necessary to switch to a competitive binding method to obtain K_{Dapp} values from SLBs containing 7.5 to 20 mol % POPS (Figure 4). Such methods are routinely applied to measuring the binding affinity of transition metal ions to proteins and peptides when the binding constant is below the nM level.[26–28] For the experiments performed here, 10 μM of a metal ion chelator, nitrilotriacetic acid (NTA), was used to shift the binding curves into the μM concentration range where the background Cu^{2+} contamination was negligible.[27,29] In fact, in the NTA-containing buffers used in the experiments described below, observable quenching only occurred when more than 0.1 μM $CuCl_2$ was introduced into the system. The data in Figure 4 are also plotted with a logarithmic x-axis in the

DOI: 10.1021/jacs.5b03313
J. Am. Chem. Soc. 2015, 137, 7785–7792

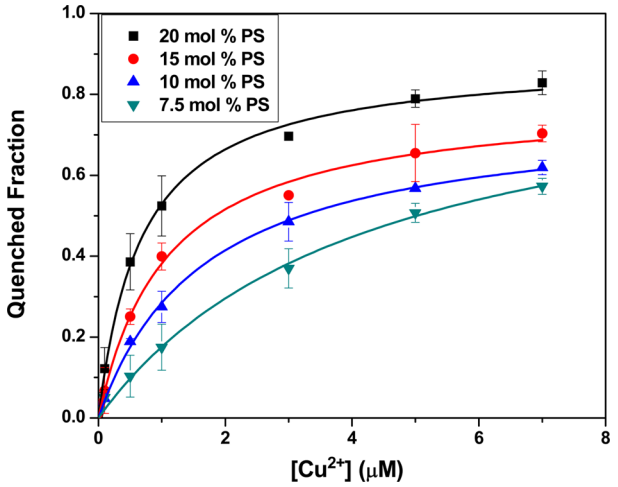

Figure 4. Quenching response of SLBs containing 1.0 mol % TR-DHPE, 7.5 to 20 mol % POPS in POPC with 10 μM NTA. The quenched fraction was normalized to the fluorescence response without Cu^{2+} at the same pH (pH = 7.4) where 400 μM EDTA was also added to the system. The solid lines represent least-squares fits of the data using eq 5. Moreover, buffers containing 1 μM NTA were also tested to confirm the K_{Dapp} values and gave similar results (Figure S4).

Supporting Information (Figure S3) to directly compare with Figure 3.

The quenching curves in Figure 4 were fit to a modified Langmuir isotherm binding model based on the available Cu^{2+} concentrations (eqs 5 and 6):

$$\Delta F = \Delta F_{max} \times \frac{[Cu^{2+}]}{[Cu^{2+}] + K_{Dcom}} \quad (5)$$

$$K_{Dcom} = K_{Dapp}\left\{1 + \frac{[NTA^{3-}]}{K_L}\right\} \quad (6)$$

Here ΔF and ΔF_{max} represent the quenched fraction of lipid-bound dye and the maximum fraction quenched, respectively. $[Cu^{2+}]$ is the Cu^{2+} concentration added into the NTA-containing buffer. K_{Dcom} is the dissociation constant extracted from the competitive binding curve when NTA is present. K_{Dapp} is the apparent dissociation constant of the Cu^{2+}–PS complex, and eq 6 shows the relationship between K_{Dcom} and K_{Dapp}. In eq 6, K_L is the NTA–Cu^{2+} binding constant at pH 7.4, which was calculated to be 10^{-10} M, based upon the known protonation constant of NTA.[30,31] The derivation of these equations is described in detail in the Supporting Information. Using eqs 5 and 6, K_{Dapp} values for PS concentrations up to 20 mol % were abstracted and are listed in the K_{Dapp} (M, competitive) column of Table 1 along with the K_{Dcom} values under each set of conditions.

To confirm that the competitive binding experiments provided accurate K_{Dapp} values, the K_{Dcom} value was obtained for membranes containing 7.5 mol % PS, a concentration that was also measured noncompetitively (Figure 3). In this case, the calculated K_{Dapp} value from competitive binding was 5.1×10^{-11} M, which differs by a factor of less than 3 from the noncompetitive binding measurements. One might have wished to use the competitive binding method to compare dissociation constants with even lower concentrations of POPS. However, K_{Dcom} values under those circumstances were larger than 10 μM. Unfortunately, introducing more than 10 μM Cu^{2+} exceeds the metal-buffering capacity of the 10 μM NTA solution. Therefore, the NTA-based competitive binding method was only used for the range of POPS concentrations from 7.5 to 20 mol %.

Characterization of the Surface Charge in the Presence of the Cu^{2+}–PS Complex. The data in Figures 3 and 4 were fit to Langmuir isotherms that assume non-cooperative binding. This assumption is unusual for cation binding at an interface. Indeed, cation binding would normally be expected to be anticooperative because early binding events would normally make subsequent ones less favorable due to increasing electrostatic repulsion. For example, Ca^{2+} and Mg^{2+} bind with phosphate and carboxyl groups on PS[19,32,33] and this attenuates and eventually reverses the negative charge on the bilayer at sufficiently high concentrations.[9,18] This is not expected to be the case for Cu^{2+}–PS binding where two protons should be released for every Cu^{2+} that binds bivalently to phosphatidylserine (Figure 1). To verify this, vibrational sum frequency spectroscopy (VSFS) experiments were performed to probe the extent of interfacial water structure that was present after Cu^{2+} and Ca^{2+} binding, which is linked to surface charge.[34−36]

VSFS measurements were made in the CH and OH stretch region of the vibrational spectrum with 100 μM $CuCl_2$ and 100 μM $CaCl_2$ in the aqueous subphase below a Langmuir monolayer of DPPS lipids (Figure 5). The sharper peaks at

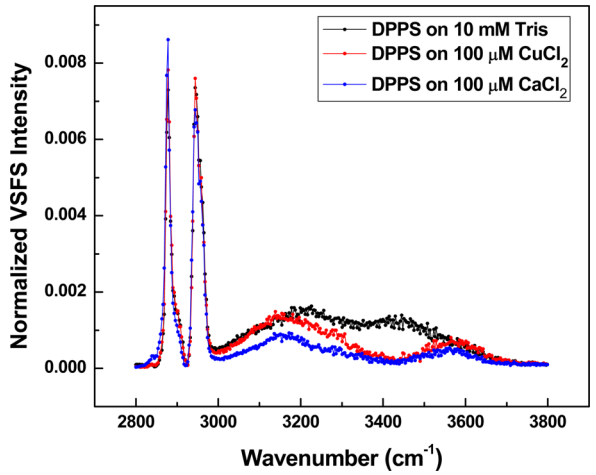

Figure 5. VSFS spectra of DPPS monolayers with 100 μM $CuCl_2$ (red data points) and 100 μM $CaCl_2$ (blue data points) in the subphase. The spectrum of a DPPS monolayer with a 10 mM Tris buffer without any divalent metal salts is shown for comparison (black data points). All measurements were made at pH 7.4 with a surface pressure of 17 mN/m at 21 °C. The fitting of the spectra is described in the Supporting Information, and the fitting results are listed in Table S1.

2880 and 2950 cm^{-1} are CH stretch modes from the lipid acyl chains,[36,37] while the broader peaks at 3200 and 3400 cm^{-1} are OH stretches arising from the alignment of interfacial water adjacent to the monolayer.[38] The peak assignments can be found in Table S1. The oscillator strength in the OH stretch region at 3200 cm^{-1} has been shown to vary with the interfacial potential for monolayers composed of lipids, surfactants, and macromolecules.[34,36,39] Specifically, highly charged surfaces order more water molecules, resulting in a larger OH stretch oscillator strength.[34] The relatively large peak intensities in the OH stretch region in the absence of added divalent metal cations (black data points in Figure 5) come from the negative

DOI: 10.1021/jacs.5b03313
J. Am. Chem. Soc. 2015, 137, 7785−7792

charge on the lipid layer. The 3200 cm^{-1} peak is expected to be attenuated by the addition of metal cations if the interfacial potential is reduced. Indeed, the oscillator strength of this resonance decreased 48% upon the introduction of 100 μM Ca^{2+} (blue data points in Figure 5). By contrast, the addition of 100 μM Cu^{2+} only causes a reduction of 7% in the oscillator strength of the 3200 cm^{-1} peak (red data points in Figure 5). The much greater attenuation of this resonance upon the introduction of Ca^{2+} is consistent with the significantly greater attenuation of the negative charge.[40] The more modest change upon the addition of Cu^{2+} supports the idea that the surface charge is less perturbed upon Cu^{2+} binding. It should be noted that a slight attenuation in the 3200 cm^{-1} resonance might be expected with 100 μM Cu^{2+} because this concentration is sufficiently high to lead to some Cu^{2+} binding with the negatively charged phosphate moieties even after all the amine sites are bound. Also, the 3400 cm^{-1} resonance was strongly perturbed by both Ca^{2+} and Cu^{2+} as this resonance reflects aligned water molecules directly bound to the lipid headgroup, which should be perturbed by divalent cation binding.[40,41]

DISCUSSION

Change of Cu^{2+}–PS Binding Affinity with PS Density.

As demonstrated above, the apparent affinity of Cu^{2+} for SLBs increased by a factor of 17 000 as the concentration of POPS was increased from 1.0 to 20 mol %. Below, we explore the extent to which this enhancement was caused by an increase in binding valency versus an increase in the surface potential. To begin, the K_{Dapp} value as a function of POPS concentration was fit to eq 1, which takes into account the extent of monovalent vs bivalent Cu^{2+} binding (Figure 6A). As can be seen, the best fit of eq 1 to the data (red line in Figure 6A) is extremely poor. The change in apparent binding is far too great to be explained by binding valency changes alone. Indeed, the charge on the surface was also increased 20-fold as the POPS concentration was raised from 1.0 to 20 mol %. This caused a large change in the interfacial potential in the double layer, which can be quantified by using the Grahame equation (eq 7).[8]

$$\sigma = 0.117\sinh\left(\frac{\psi_0}{51.4}\right) \times \left\{[\mathrm{Tris}^+] + [\mathrm{CuCl_2}]\left[2 + \exp\left(\frac{-\psi_0}{25.7}\right)\right]\right\}^{1/2} \quad (7)$$

where σ is the surface charge density (C/m^2), ψ_0 is the surface potential (mV), and $[Tris^+]$ and $[CuCl_2]$ are the concentrations of protonated Tris and $CuCl_2$ in the buffer (M). The derivation of eq 7 can be found in ref 8. The surface charge density, σ, can be determined by using eq 8:

$$\sigma = \frac{-e}{S} \times (\chi_{PS} + \chi_{TR}) \quad (8)$$

where the lipid headgroup area, S, was taken to be 70 Å^2[42] and e is the fundamental unit of charge. Moreover, χ_{PS} and χ_{TR} represent the mole fractions of POPS and TR-DHPE in the SLBs, respectively. This calculation takes into account the fact that both the TR-DHPE and POPS possess a net charge of −1. The calculated σ values are provided in Table 2 and were plugged into eq 7 to solve for ψ_0. Using the surface potential, ψ_0, together with the K_{Dapp} values measured in Figures 3 and 4, it is possible to calculate the intrinsic dissociation constant, K_{Dint} (eq 9):[8,9]

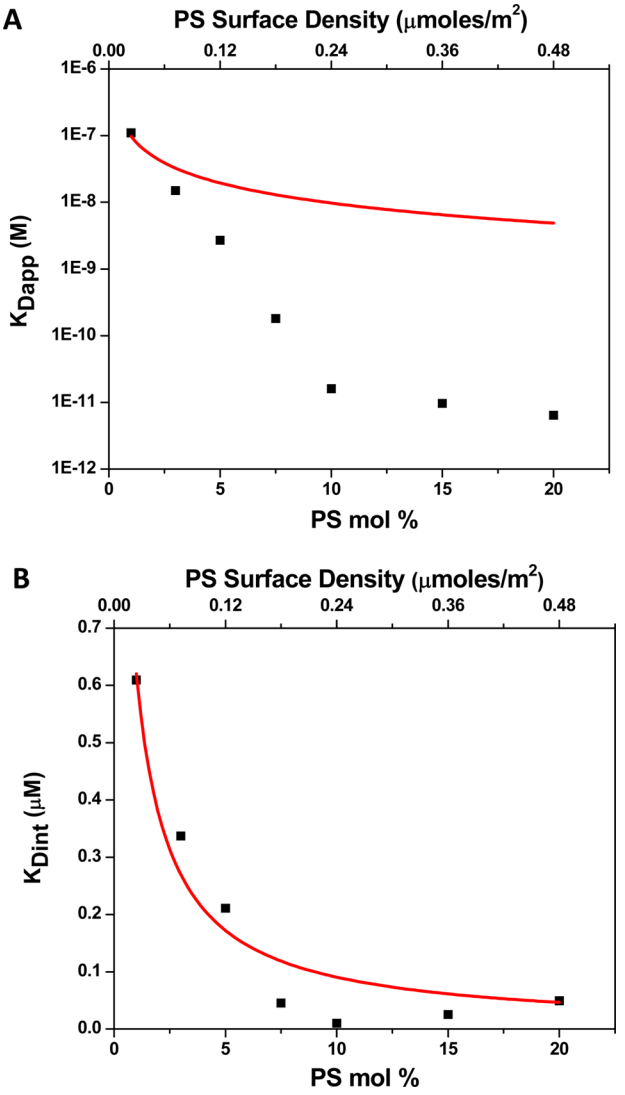

Figure 6. (A) K_{Dapp} values and (B) K_{Dint} values plotted as a function of POPS surface density. The data points (black dots) are plotted as POPS surface density in units of μmol/m^2 (top x-axis) and POPS mol % (bottom x-axis). The red lines in each panel are best fits of eq 1 to the data. To clearly present the data points and the fitted curves, the y-axis in (A) is plotted as a logarithmic scale while the y-axis in (B) is linear. The curve in Figure 6A does not fit the data, as the change in K_{Dapp} is far too great to be fit by a change in binding valency alone (eq 1).

Table 2

PS mol %	σ (C/m^2)	Ψ_0 (mV)	K_{Dint} (M)
1.0	-4.6×10^{-3}	−22	6.1×10^{-7}
3.0	-9.1×10^{-3}	−40	3.4×10^{-7}
5.0	-1.4×10^{-2}	−56	2.1×10^{-7}
7.5	-1.9×10^{-2}	−71	4.5×10^{-8}
10	-2.5×10^{-2}	−83	1.0×10^{-8}
15	-3.7×10^{-2}	−101	2.5×10^{-8}
20	-4.8×10^{-2}	−115	4.9×10^{-8}

$$K_{Dint} = K_{Dapp} \times \exp\left(\frac{-2e\psi_0}{kT}\right) \quad (9)$$

The calculated K_{Dint} values are listed in Table 2 and take into account the adjustment of K_{Dapp} for a given value of the surface

DOI: 10.1021/jacs.5b03313
J. Am. Chem. Soc. 2015, 137, 7785−7792

potential. As can be seen, the K_{Dint} values only tightened by a factor of 12 between 1 and 20 mol % POPS.

Figure 6B plots K_{Dint} as a function of POPS density in the membrane (black squares). The red curve is the best fit to these data using eq 1. By contrast with Figure 6A, it can be seen that Figure 6B is satisfactorily fit by this equation. The roughly 1 order of magnitude change in K_{Dint} occurs because the binding changes from predominantly monovalent at low POPS concentration to overwhelmingly bivalent at 20 mol %. The bivalent Cu^{2+}–PS binding is assumed to occur in two sequential steps that have individual dissociation constants K_{D1} and K_{D2}, respectively. The best-fit values for these constants (red curve in Figure 6B) are 1.8 μM and 0.026 μmol/m^2, respectively. Since K_{Dint} changes by only a factor of 12 with POPS density, there is another factor of roughly 1400 in K_{Dapp} that should stem from the increase in surface potential as the membrane is made more negatively charged (eq 9).

Since Cu^{2+} can bind monovalently or bivalently to POPS, two different limiting case scenarios need to be considered to appreciate the greater than 3 orders of magnitude change in K_{Dapp} which arises as the surface charge is increased. First, for monovalent binding, the resulting Cu(PS) complex would be neutral because of the displacement of a proton upon ion binding. In this case, the membrane would have half its surface charges quenched at a bulk Cu^{2+} concentration equal to K_{Dapp}. If, hypothetically, Cu^{2+} only bound monovalently to a membrane containing 20 mol % POPS, then the surface potential would be reduced from −115 mV to −83 mV under the conditions of these experiments (Table 2). This would still produce a 175-fold enhancement of K_{Dapp} due to the surface potential. Alternatively, if Cu^{2+} bound bivalently to POPS, but did not undergo deprotonation of the amine, the membrane would also still bear half its charge at a bulk Cu^{2+} concentration equal to K_{Dapp}. Therefore, again one would expect a 175-fold tightening of K_{Dapp} from the surface potential as the POPS concentration was raised from 1.0 to 20 mol %, even if Cu^{2+} could not deprotonate the amine. The additional value of deprotonation, therefore, is worth approximately a factor of 8 out of a factor of 1400 that is attributed to the electrostatic portion of the binding enhancement.

The lack of change in the surface charge upon Cu^{2+} binding to PS is different from the binding of other divalent cations such as Ca^{2+} and Mg^{2+}.[9,18,20] It has been shown that Ca^{2+} binds primarily in a monovalent fashion with PS and does not deprotonate the amine upon binding to PS head groups.[9] The saturation binding of Ca^{2+} to PS in the bilayer actually leads to a complete inversion of the charge at a saturation concentration of Ca^{2+}. Moreover, the surface charge should be zero at the point where the bulk Ca^{2+} concentration is equal to K_{Dapp}. Under these conditions, K_{Dapp} is equal to K_{Dint}.

It should be noted that while bivalent binding of Cu^{2+} only directly leads to a modest enhancement of binding avidity with POPS, it is of indirect importance because it leads to less quenching of the surface charge than monovalent binding. Also, one may wonder why Cu^{2+} binding can be predominantly bivalent at higher concentrations of PS, while Ca^{2+} remains overwhelmingly monovalent. The reason should be related to the tight binding between the transition metal ion and the amine groups,[43] whereas Ca^{2+} can only bind electrostatically with either the carboxyl or phosphate groups.[19,32,33] The K_{D1} value for the Cu^{2+}–PS complex found here, 1.8 μM, is approximately 4 orders of magnitude tighter than the monovalent binding between Ca^{2+} and PS.[9] If it was assumed that the K_{D2} value for the Ca^{2+}–PS complex is also several orders of magnitude weaker than that for the Cu^{2+}–PS complex, then little bivalent binding should be expected for Ca^{2+} even when the membrane consists of 100 mol % PS. Indeed, that is exactly what has been previously found.[9] Nevertheless, it is curious to note that Ca^{2+} binding to membranes can lead to domain formation.[44]

Physiological Implications of Cu^{2+}–PS Binding. As the third most abundant transition metal in the human body, copper is necessary for the activity of various proteins and is tightly regulated by chaperons and enzymes in healthy cells.[45,46] In healthy tissues, the total copper concentration can be around 0.1 mM[45] and there is little uncomplexed copper (~10^{-18} M) in the cytoplasm.[47] This can change in diseased tissue. Previous reports concerning the unbound copper concentration in the cytoplasm are mainly based on studies in bacteria and yeast.[47] It has been argued that the situation in higher organisms with specialized tissues such as the human nervous systems might be different, especially under specific pathological conditions.[45] For example, it has been found that a buildup of labile Cu^{2+} is probably toxic to cells and may be linked to neurodegenerative disorders such as Wilson's disease and Alzheimer's disease.[46,48]

Various approaches have been employed to study Cu^{2+}–protein interactions, and Cu^{2+} is generally found to bind negatively charged moieties on proteins as well as the lone electron pairs of nitrogen on histidine, lysine, arginine, and the *N*-terminus.[49−52] By contrast, there has been little discussion as to how Cu^{2+} interacts with lipids or the possibility of lipid membranes serving as metal ion reservoirs when copper homeostasis breaks down. The interactions between Cu^{2+} and PS may directly affect the physical properties of the membrane. It has been shown that Cu^{2+} can destabilize multilamellar lipid vesicles at very high metal ion concentrations and change the membrane fluidity.[53,54] These changes have been suggested to occur due to domain formation induced by Cu^{2+} binding to the phosphate moiety on lipid head groups at mM Cu^{2+} concentrations.[53] By contrast, no evidence of domain formation was found in the work presented here, where the primary interactions should be with the amine and carboxylate moieties. Indeed, the 2 PS to 1 Cu^{2+} complex formed in the pM to μM range has a charge of −2. As such, bivalent Cu^{2+}–PS complexes should be electrostatically repulsive, making domain formation unlikely. Moreover, no domains should be formed under the typical physiological concentrations of Cu^{2+} around cell membranes, which is 1 to 10 μM.[45]

In addition to changes in the physical properties of lipid membranes, Cu^{2+} binding might also disrupt PS-dependent protein–membrane binding. For example, Cu^{2+} has been found to enhance the association of Aβ with mixed PC/PS bilayer systems.[53] Moreover, the oxidative damage of cell membranes containing polyunsaturated fatty acids (PUFA) could also be enhanced when copper ions, which are redox active, are attracted to the membrane surface.[13,55,56] The consequences of these interactions are probably more pronounced when PS is flipped from the inner to the outer leaflet of plasma membranes during cell apoptosis or other biological events, which increases the exposed PS density on cell surfaces and brings PS into direct contact with a Cu^{2+}-rich environment.[57,58] With a relatively high negatively charged PS density on the cell surface, the apparent binding affinity to Cu^{2+} should be enhanced, which would make PS a putative copper ion reservoir.

DOI: 10.1021/jacs.5b03313
J. Am. Chem. Soc. 2015, 137, 7785−7792

■ ASSOCIATED CONTENT

Supporting Information

Supporting materials include the Experimental Section; a schematic diagram of the experiment setup; the table of the fitted oscillator strengths and widths of the VSFS spectra peaks; the binding curves for POPC SLBs containing 5.0 mol % POPS, DPPS and DOPS; the derivation of the equations for the NTA competitive binding method; the competitive binding curves with 10 μM NTA shown on linear and logarithmic x-axes; the competitive binding curves with 1 μM vs 10 μM NTA; and the details of the calculations of σ, ψ_0, and K_{Dint}. The Supporting Information is available free of charge on the ACS Publications website at DOI: 10.1021/jacs.5b03313.

■ AUTHOR INFORMATION

Corresponding Author

*psc11@psu.edu

Notes

The authors declare no competing financial interest.

■ ACKNOWLEDGMENTS

We thank Dr. William D. James (Elemental Analysis Laboratory, Texas A&M University) for the assistance with inductively coupled plasma mass spectrometry (ICP-MS) to test for contamination by copper ions in the buffer. We also wish to thank Professor Amie Boal and Dr. Tinglu Yang at Penn State for helpful discussions and Mr. Dongyue Xin at Texas A&M for his help in figure preparation. This work was funded by the National Institutes of Health (Grant GM070622), the Office of Naval Research (Grant N00014-08-1-0467), and the Robert A. Welch Foundation (Grant A-1421).

■ REFERENCES

(1) Mammen, M.; Choi, S. K.; Whitesides, G. M. *Angew. Chem., Int. Ed.* **1998**, *37*, 2755.
(2) Jayaraman, N. *Chem. Soc. Rev.* **2009**, *38*, 3463.
(3) Rihova, B. *Adv. Drug Delivery Rev.* **1998**, *29*, 273.
(4) Heldin, C. H. *Cell* **1995**, *80*, 213.
(5) Yang, T. L.; Baryshnikova, O. K.; Mao, H. B.; Holden, M. A.; Cremer, P. S. *J. Am. Chem. Soc.* **2003**, *125*, 4779.
(6) Shi, J.; Yang, T.; Kataoka, S.; Zhang, Y.; Diaz, A. J.; Cremer, P. S. *J. Am. Chem. Soc.* **2007**, *129*, 5954.
(7) Leckband, D. E.; Kuhl, T.; Wang, H. K.; Herron, J.; Muller, W.; Ringsdorf, H. *Biochemistry* **1995**, *34*, 11467.
(8) Israelachvili, J. N. *Intermolecular and Surface Forces*, 3rd ed.; Academic Press: 2011; p 1.
(9) Mclaughlin, S.; Mulrine, N.; Gresalfi, T.; Vaio, G.; Mclaughlin, A. *J. Gen. Physiol.* **1981**, *77*, 445.
(10) Jung, H.; Robison, A. D.; Cremer, P. S. *J. Struct. Biol.* **2009**, *168*, 90.
(11) Pisarchick, M. L.; Thompson, N. L. *Biophys. J.* **1990**, *58*, 1235.
(12) Kalb, E.; Engel, J.; Tamm, L. K. *Biochemistry* **1990**, *29*, 1607.
(13) Leventis, P. A.; Grinstein, S. *Annu. Rev. Biophys* **2010**, *39*, 407.
(14) Gordesky, S. E.; Marinett, G. V. *Biochem. Biophys. Res. Commun.* **1973**, *50*, 1027.
(15) Li, M. O.; Sarkisian, M. R.; Mehal, W. Z.; Rakic, P.; Flavell, R. A. *Science* **2003**, *302*, 1560.
(16) Zwaal, R. F. A.; Comfurius, P.; Bevers, E. M. *Bioch. Biophys. Acta, Rev. Biomembranes* **1998**, *1376*, 433.
(17) Huang, B. X.; Akbar, M.; Kevala, K.; Kim, H. Y. *J. Cell Biol.* **2011**, *192*, 979.
(18) Hauser, H.; Darke, A.; Phillips, M. C. *Eur. J. Biochem.* **1976**, *62*, 335.
(19) Shirane, K.; Kuriyama, S.; Tokimoto, T. *Biochim. Biophys. Acta* **1984**, *769*, 596.
(20) Newton, C.; Pangborn, W.; Nir, S.; Papahadjopoulos, D. *Biochim. Biophys. Acta* **1978**, *506*, 281.
(21) Hendrickson, H. S.; Fullington, J. G. *Biochemistry* **1965**, *4*, 1599.
(22) Monson, C. F.; Cong, X.; Robison, A. D.; Pace, H. P.; Liu, C. M.; Poyton, M. F.; Cremer, P. S. *J. Am. Chem. Soc.* **2012**, *134*, 7773.
(23) Lakowicz, J. R. *Principles of Fluorescence Spectroscopy*, 3rd ed.; Springer Science+Business Media: New York, 2006.
(24) Matthews, J. C. *Fundamentals of Receptor, Enzyme, and Transport Kinetics*; CRC Press: Boca Raton, FL, 1993.
(25) Tamm, L. K.; Bartoldus, I. *Biochemistry* **1988**, *27*, 7453.
(26) Zhang, L.; Koay, M.; Mahert, M. J.; Xiao, Z.; Wedd, A. G. *J. Am. Chem. Soc.* **2006**, *128*, 5834.
(27) Atwood, C. S.; Scarpa, R. C.; Huang, X. D.; Moir, R. D.; Jones, W. D.; Fairlie, D. P.; Tanzi, R. E.; Bush, A. I. *J. Neurochem.* **2000**, *75*, 1219.
(28) Perrin, D. D.; Dempsey, B. *Buffers for pH and Metal Ion Control*; Chapman and Hall; Wiley: London, NY, 1974.
(29) Sarell, C. J.; Syme, C. D.; Rigby, S. E. J.; Viles, J. H. *Biochemistry* **2009**, *48*, 4388.
(30) Anderegg, G. *Pure Appl. Chem.* **1982**, *54*, 2693.
(31) Motekaitis, R. J.; Martell, A. E. *J. Coord. Chem.* **1994**, *31*, 67.
(32) Pedersen, U. R.; Leidy, C.; Westh, P.; Peters, G. H. *Biochim. Biophys. Acta, Biomembranes* **2006**, *1758*, 573.
(33) Bockmann, R. A.; Grubmuller, H. *Angew. Chem., Int. Ed.* **2004**, *43*, 1021.
(34) Richmond, G. L. *Chem. Rev.* **2002**, *102*, 2693.
(35) Shen, Y. R. *Nature* **1989**, *337*, 519.
(36) Kim, J.; Kim, G.; Cremer, P. S. *Langmuir* **2001**, *17*, 7255.
(37) Chen, X.; Yang, T.; Kataoka, S.; Cremer, P. S. *J. Am. Chem. Soc.* **2007**, *129*, 12272.
(38) Shen, Y. R.; Ostroverkhov, V. *Chem. Rev.* **2006**, *106*, 1140.
(39) Schultz, Z. D.; Levin, I. W. *Ann. Rev. Anal. Chem.* **2011**, *4*, 343.
(40) Chen, X. K.; Hua, W.; Huang, Z. S.; Allen, H. C. *J. Am. Chem. Soc.* **2010**, *132*, 11336.
(41) Covert, P. A.; Jena, K. C.; Hore, D. K. *J. Phys. Chem. Lett.* **2014**, *5*, 143.
(42) White, S. H.; King, G. I. *Proc. Natl. Acad. Sci. U.S.A.* **1985**, *82*, 6532.
(43) Martell, A. E.; Motekaitis, R. J. *Determination and use of stability constants*, 2nd ed.; VCH Publishers: New York, 1992.
(44) Boettcher, J. M.; Davis-Harrison, R. L.; Clay, M. C.; Nieuwkoop, A. J.; Ohkubo, Y. Z.; Tajkhorshid, E.; Morrissey, J. H.; Rienstra, C. M. *Biochemistry* **2011**, *50*, 2264.
(45) Que, E. L.; Domaille, D. W.; Chang, C. J. *Chem. Rev.* **2008**, *108*, 1517.
(46) Gaggelli, E.; Kozlowski, H.; Valensin, D.; Valensin, G. *Chem. Rev.* **2006**, *106*, 1995.
(47) Rae, T. D.; Schmidt, P. J.; Pufahl, R. A.; Culotta, V. C.; O'Halloran, T. V. *Science* **1999**, *284*, 805.
(48) Bush, A. I. *Trends Neurosci.* **2003**, *26*, 207.
(49) Makinen, W. B.; Pearlmut, A. F.; Stuehr, J. E. *J. Am. Chem. Soc.* **1969**, *91*, 4083.
(50) Smith, D. P.; Smith, D. G.; Curtain, C. C.; Boas, J. F.; Pilbrow, J. R.; Ciccotosto, G. D.; Lau, T. L.; Tew, D. J.; Perez, K.; Wade, J. D.; Bush, A. I.; Drew, S. C.; Separovic, F.; Masters, C. L.; Cappai, R.; Barnham, K. J. *J. Biol. Chem.* **2006**, *281*, 15145.
(51) Lavanant, H.; Hoppilliard, Y. *Eur. J. Mass Spectrom.* **1999**, *5*, 41.
(52) Hong, L. A.; Carducci, T. M.; Bush, W. D.; Dudzik, C. G.; Millhauser, G. L.; Simon, J. D. *J. Phys. Chem. B* **2010**, *114*, 11261.
(53) Lau, T. L.; Ambroggio, E. E.; Tew, D. J.; Cappai, R.; Masters, C. L.; Fidelio, G. D.; Barnham, K. J.; Separovic, F. *J. Mol. Biol.* **2006**, *356*, 759.
(54) Gehman, J. D.; O'Brien, C. C.; Shabanpoor, F.; Wade, J. D.; Separovic, F. *Eur. Biophys. J. Biophys. Lett.* **2008**, *37*, 333.
(55) Gal, S.; Lichtenberg, D.; Bor, A.; Pinchuk, I. *Chem. Phys. Lipids* **2007**, *150*, 186.
(56) Gaetke, L. M.; Chow, C. K. *Toxicology* **2003**, *189*, 147.

DOI: 10.1021/jacs.5b03313
J. Am. Chem. Soc. 2015, 137, 7785−7792

(57) Bratton, D. L.; Fadok, V. A.; Richter, D. A.; Kailey, J. M.; Guthrie, L. A.; Henson, P. M. *J. Biol. Chem.* **1997**, *272*, 26159.
(58) Balasubramanian, K.; Mirnikjoo, B.; Schroit, A. J. *J. Biol. Chem.* **2007**, *282*, 18357.

DOI: 10.1021/jacs.5b03313
J. Am. Chem. Soc. 2015, 137, 7785−7792